Molecular Model of Dimethylmethylphosphonate and Its Interactions with Water

Aleksey Vishnyakov and Alexander V. Neimark*

Center for Modeling and Characterization of Nanoporous Materials, TRI/Princeton, 601 Prospect Avenue, Princeton, New Jersey 08542

Received: June 16, 2003; In Final Form: November 3, 2003

We propose a simple united-atom second-order potential model for dimethylmethylphosphonate (DMMP) designed to reproduce molecular conformations and physical properties, such as the liquid density, heat of evaporation, and thermal expansion coefficient of the pure liquid. By use of the model, we explore molecular structure, thermodynamic characteristics, and dynamic properties of liquid DMMP and its aqueous solutions by molecular dynamics simulations. It is shown that accurate choice of partial atomic charges is of crucial importance for a correct description of phase behavior and physical properties of aqueous solutions of alkylphosphonates. The excess volume and the enthalpy of mixing in a DMMP−water system were found negative with a minimum presumably located within the concentration range between 33 and 50% volume. On average, one DMMP molecule forms two hydrogen bonds with surrounding water via the oxygen atom that forms a double bond to phosphorus. The average lifetime of hydrogen bonds does not exceed rotation correlation time of individual water molecule, thus indicating that there are no long-living DMMP·H_2O complexes in the aqueous solutions.

1. Introduction

Dimethylmethylphosphonate (DMMP, Figure 1), one of the simplest alkylphosphonates, is often used in chemical research as a relatively nontoxic model substance to mimic properties of organophosphorus nerve agents (see, e.g., refs 1−3). This work was motivated by the intent to study the mechanisms of transport of organophosphorus compounds through permselective polyelectrolite membranes (PEM) by means of molecular simulations. PEM are expected to be used in new protective materials. However, the application of molecular simulation methods to alkylphosphonates is hindered by the absence of a simple yet accurate molecular model.

In the present paper, we suggest a simple potential model for DMMP that (i) reproduces the conformations of DMMP molecule in a vacuum obtained by ab initio modeling;[4] (ii) is in good agreement with experimental data on physical properties of pure liquid, such as the density at ambient conditions, the heat of evaporation, and the thermal expansion coefficient; and (iii) gives a qualitatively reasonable physical picture of DMMP−water interactions in binary solutions. The molecular models are described in Section 2. The thermodynamic properties and the molecular structure of pure DMMP and its aqueous solutions are discussed in Sections 3 and 4, respectively.

2. Molecular Models

Unlike alkyl phosphate groups that are found in biological macromolecules, alkylphosphonates received relatively little attention from both experimentalists and theoreticians. Thermodynamic and dielectric properties of lower alkylphosphonates including DMMP were studied back in 50s.[5−8] The dielectric constants obtained allowed to speculate on preferential conformations of lower alkylphosphonates; in particular, "extended" and "folded" (described below) geometries were considered.[6,7]

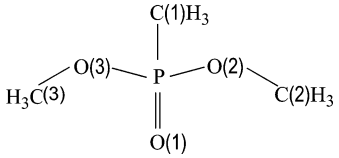

Figure 1. Dimethylmethylphosphonate molecule. Numbering of nonhydrogen atoms given in the brackets.

Recently, Suenram et al.[4] thoroughly studied the conformations of DMMP molecules in a vacuum using Fourier transform microwave spectroscopy and ab initio Hartree−Fock (HF) and Møller−Plesset (MP2) calculations. Two preferential conformations, separated by a shallow potential barrier, were detected. The lowest potential energy corresponds to an asymmetric conformation (further on referred to as conformer A) shown in Figure 2a. The other preferential conformation is symmetric (denoted as conformer B, Figure 2b); it corresponds to the "extended" conformation discussed in refs 6 and 7.

Simulations of alkylphosphonates published in the literature[9−13] employed generic force fields such as CHARMM,[14] AMBER,[15] and UFF.[16] Terms specific to phosphonates were also incorporated into generic force fields.[9−11,13] However, a detailed analysis of the properties of simpler homologues with verification against available experimental data limits is an essential step toward reliable force fields applicable to complex molecules, while application of a generic force field may be misleading. In particular, minimization of the potential energy of DMMP based on the UFF force field and the partial charges obtained using the Gasteiger procedure[17] yielded two major conformers that qualitatively resemble those observed in ref 4. However, in a disagreement with the ab initio results, the UFF conformers have almost ideal trans and gauche dihedral angles. Also, the symmetric conformer is ca. 7.1 kJ/mol less stable than the asymmetric one.

We developed a new potential model for DMMP via an iteration procedure that included static energy optimization of

* Author to whom correspondence should be addressed. E-mail: aneimark@triprinceton.org.

10.1021/jp035708p CCC: $27.50
Published on Web 02/03/2004

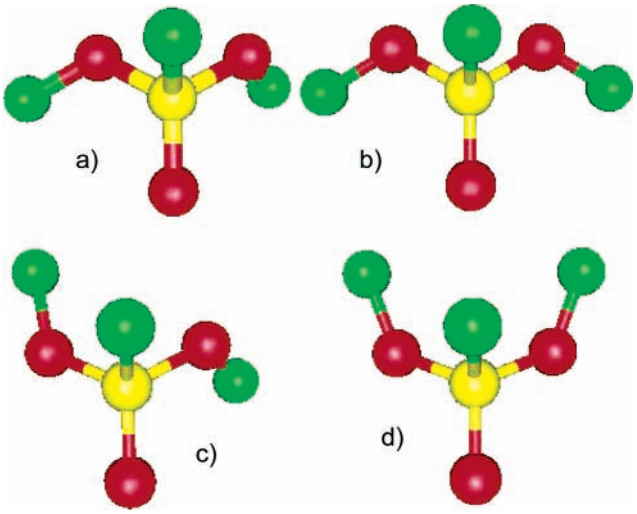

Figure 2. Four potential minima of DMMP molecule obtained by the potential-energy minimization with Model 2 (a) conformation A, which corresponds to the deepest minimum of the potential energy and the preferential conformation in liquid DMMP, (b) conformation B, found frequently in liquid DMMP, "extended" conformation in refs 6 and 7, and (c, d) conformations C and D, local energy minima with higher potential energies, conformation D is referred to as "folded" in refs 6 and 7. Visualization using gOpenMol 2.0 [31]

TABLE 1: Geometry of DMMP Molecule Obtained by Molecular Mechanics with Classical Model 2 (This Work) and by ab initio Modeling (Ref 4)

	conformer A			conformer B	
	HF [4]	model 1	model 2	model 1	model 2
		Bond (Å)			
P_1-C_1	1.795	1.797	1.801	1.796	1.796
P_1-O_1	1.458	1.458	1.458	1.459	1.459
P_1-O_2	1.594	1.592	1.595	1.589	1.589
P_1-O_3	1.581	1.590	1.590	1.589	1.589
O_4-C_2	1.419	1.421	1.423	1.420	1.420
O_6-C_3	1.418	1.418	1.419	1.420	1.420
		Angle			
$C_1-P_1-O_1$	116.1	115.3	112.9	114.7	114.7
$C_1-P_1-O_2$	101.5	102.7	101.8	101.7	101.9
$C_1-P_1-O_3$	105.8	103.9	103.5	101.7	101.9
$O_1-P_1-O_2$	113.2	115.4	110.4	116.2	116.0
$O_1-P_1-O_3$	116.2	116.2	115.5	116.2	116.0
$O_2-P_1-O_3$	102.8	101.4	105.9	104.4	104.7
$P_1-O_2-C_2$	121.1	121.3	122.0	122.6	122.5
$P_1-O_3-C_3$	121.9	121.9	122.6	122.6	122.5
		Torsion Angle			
$C_1-P_1-O_2-C_2$	103.1	109.7	105.0	161.1	160.1
$C_1-P_1-O_3-C_3$	175.9	170.5	170.0	161.1	160.1
$O_1-P_1-O_2-C_2$	25.1	18.1	21.2	36.0	34.9
$O_1-P_1-O_3-C_3$	48.9	44.3	45.5	36.0	34.9
$O_2-P_1-O_3-C_3$	74.9	82.2	82.1	93.3	94.3
$O_3-P_1-O_2-C_2$	151.0	144.0	148.2	93.3	94.3

a single DMMP molecule in a vacuum and probe MD simulations of liquid DMMP. Simple quadratic functions were used for covalent-bond-stretching and angle-bending potentials, $U_{bond}(r) = F_{bond}(r - r_0)^2$ and $U_{angle}(\theta) = F_{angle}(\theta - \theta_0)^2$, where r_0 and θ_0 are the equilibrium bond length and angle. The values of r_0 and θ_0 were chosen to fit the ab initio bond lengths and angles from ref 4. The torsion potentials for dihedral angles were fitted using the standard functions $\Psi_{tors}(\theta) = \Sigma_{i=1}^{N} V_i(1 + \cos(\theta))$ with $N = 6$. Considerable differences between the dihedral angles of conformer A (Table 1) and the locations of minima of standard dihedral potentials show the importance of the choice of a scaling factor 1−4 nonbonded interactions (i.e., interactions between the atoms separated by three covalent bonds). We chose the scaling factor of 0.5, which is a standard factor in several generic force fields. At the zero value of the scaling factor, the conformation tended to be idealized, with distinct trans and gauche torsion angles, while at the scaling factor of 1 the model tended to prefer conformer B because of the Lennard-Jones repulsion between the CH_3 groups. The scaling factor for 1−5 nonbonded interactions (in this case, between C2 and C3 atoms) was equal to 1.

TABLE 2: Parameters of the Force Field for DMMP

Nonbonded Parameters (LJ and Partial Charges)

	model 1 (charges obtained using Gasteiger[17] method)			model 2 (charges match the experimental dipole moment)		
atom	σ, Å	ϵ, kJ/mol	q, e	σ, Å	ϵ, kJ/mol	q, e
P_O (P_1)	3.831	2.451	1.1736	3.83	1.451	1.17
O_P (O_1)	3.030	0.637	−0.536	2.93	0.667	−0.691
C_{CH_3P} (C_1)	3.775	0.677	0.0278	3.80	0.865	−0.021
O_{CH_3} (O_2, O_3)	3.153	0.637	−0.485	3.03	0.667	−0.36
C_{CH_3O} (C_2, C_3)	3.775	0.677	0.153	3.80	0.865	0.135

Equilibrium Bond Lengths, Å

P_O-O_P 1.458 P_O-C_P 1.795 $P_O-O_{CH_3}$ 1.586 $O_{CH_3}-C_{CH_3O}$ 1.418

Covalent Angles

angle	θ_0, deg	F, kJ/deg^2 mol	angle	θ_0, deg	F, kJ/deg^2 mol
$O_P-P_O-C_P$	116.3	335.	$C_P-P_O-O_{CH_3}$	104.3	170.
$O_P-P_O-O_{CH_3}$	116.5	419.0	$P_O-O_{CH_3}-C_{CH_3O}$	121.0	335.

Torsion Angles, V_i (kJ/mol)

angle	V_1	V_2	V_3	V_4	V_5	V_6
$C_P-P_O-O_{CH_3}-C_{CH_3O}$	0.281	2.633	0.316	−0.244	0.307	−0.025
$O_P-P_O-O_{CH_3}-C_{CH_3O}$			0.42			
$O_{CH}-P_O-O_{CH_3}-C_{CH_3}$		3.99	2.1			

The iteration procedure started from the CHARMM potential for alkyl phosphates.[14] Then the C−P−O−C torsion potential was fitted in order to reproduce roughly the required conformer A (see Figure S1 in Supporting Information). On each iteration step, we changed the torsion parameters in order to get closer to the required geometry of conformer A and make it slightly more stable than conformer B. Then the Lennard-Jones parameters were scaled in order to obtain reasonable liquid density and the heat of evaporation.

We performed the iteration procedure for two sets of partial atomic charges (Table 2). The difference in charges caused a visible difference in resulted LJ parameters but very little difference in torsion parameters, which are identical in the two models. The first set of the atomic charges (further on referred to as model 1) was obtained using the Gasteiger procedure. Similar charges were produced using the charge−equilibration procedure implemented in Cerius2.[18] However, model 1 does not reproduce the dipole moment of the molecule. In ref 7, the dipole moment of DMMP was estimated as $\mu = 3.6$ D from the dielectric permeability using the Onsager equation. Previously, $\mu = 3.0-3.6$ D was reported based on the polarity of different bonds in DMMP molecule.[6] Buckingham's empirical approach[19] for the estimation of the dipole moment from dielectric permeabilities and molecular geometries of pure liquids[5,20] resulted in $\mu = 2.48-3.04$ D (depending on the conformation) with the approximate mean value of 2.78 D. These studies show that the dipole moment of DMMP in pure liquid is rather high, around 3.0 D, and almost coaxial with the P═O double bond. However, model 1 results in $\mu_A = 1.87$ D, $\cos(\vec{\mu},PO) = 0.5$, and $\mu_B = 1.08$ D, $\cos(\vec{\mu},PO) = 0.784$. Therefore, we employed the second set of charges and LJ parameters (model 2) in order to comply to the results of refs 6 and 8. Model 2 gives $\mu_A = 2.93$ D, $\cos(\vec{\mu},PO) = 0.94$, and

TABLE 3: Physical Properties of Pure DMMP Obtained in This Work from MD Simulations and Experimental Data[7,8]

	model 1	model 2	exp
ρ, g/cm^3, 303 K	1.1581	1.1562	1.1507
ρ, g/cm^3, 373 K	1.0772	1.0853	1.0717
ΔH_{l-v}, kJ/mol 303 K	50.94	50.11	52.25
D 10^9 m^2/s, 303 K		0.39	0.5 (at 293 K)[32]
τ_{rot} dipole 303 K		13.16	

$\mu_B = 2.73$ D, $\cos(\vec{\mu},PO) = 0.999$ ($\cos(\vec{\mu},PO) = 1$ was not a target of a fit). The final set of the LJ parameters is close to the parameters of the united-atom OPLS force field.[21] As shown below, the low dipole moment of model 1 causes a phase separation in DMMP−water solutions in contradiction with the experimental data. The results described in this paper are obtained with model 2 unless otherwise stated.

The potential-energy optimization using the force field developed (model 2) revealed four local minima of the potential energy of DMMP molecule (Figure 2). The asymmetric conformer A has the lowest potential energy. Geometry of the asymmetric conformer is in good agreement with the ab initio results,[4] as demonstrated in Table 1. Since the DMMP molecule itself has a plane of symmetry, conformer A has a mirror image of the same stability. The symmetric conformer B (Figure 2b) is just 2.0 kJ/mol less stable. The potential energies of the other two conformers C and D (parts c and d of Figure 2) are much higher, which allows us to assume that their concentrations in liquid DMMP are negligibly small.

3. Pure DMMP Liquid

Simulation Details. The MD simulations of pure DMMP were carried out at constant temperature and pressure (that is, in NPT ensemble) $T = 303$ and 403 K and $p = 1$ atm. DMMP (400 molecules) were placed in a cubic periodic basic cell with 3D periodic boundary conditions. The conformations in the initial configuration were chosen randomly. The simulation software used was the M.Dyna*Mix*4.3 package[22] obtained from Stockholm University. The equations of motion were solved using the Verlet[23] leapfrog scheme with the time step of 1 fs. Covalent bonds were constrained by the SHAKE algorithm.[24] Temperature and pressure were maintained with the Nose−Hoover[25,26] thermostat. Each system was simulated over 500 ps, and the statistics were collected during the last 250 ps. Translational diffusion coefficients were calculated from the mean square displacement (MSD) using the Einstein relationship and the velocity autocorrelation functions (VACF). Distinct regions of linearity on MSD vs time correlations were observed for all systems. The rotational mobility of molecules was characterized by reorientation and rotation correlation times τ_1 and τ_2 for the dipole vector, estimated from the corresponding autocorrelation functions $C_i(t)$, which were assumed to decay exponentially at $t > 4$ ps. The heat of vaporization was calculated from the potential energy and density of the liquid, assuming that the coexisting vapor was an ideal gas.

Thermodynamic Properties. For both models of DMMP, we have obtained good agreement with the experimental density and heat of evaporation. One could notice that the translational diffusion and the rotation mobility are fairly slow, about 1 order of magnitude lower then those of pure water. MD simulations at 373 K were performed to measure the thermal expansion coefficient. Although the model slightly overestimates the expansion, the agreement with experiment is quite reasonable (Table 3).

Molecular Structure. An analysis of the intramolecular radial distribution functions (RDF) shows that conformations A and B (Figure 2) prevail in the solution. In Figure 3a, asymmetric conformation A, where the distance between C_2 and C_3 atoms is ca. 3.95 Å, corresponds to the first peak of intramolecular RDF. Symmetric conformation B (equilibrium C_2-C_3 distance of 4.2 Å) corresponds to the first peak. Conformer A, which is more stable in a vacuum, also prevails in the liquid (Figure 3b). It is worth noting that the conformational behavior of liquids is often controlled by intermolecular interactions and may differ drastically from that in a vacuum. The "folded" conformer D discussed in refs 6 and 7 was not observed in the solution.

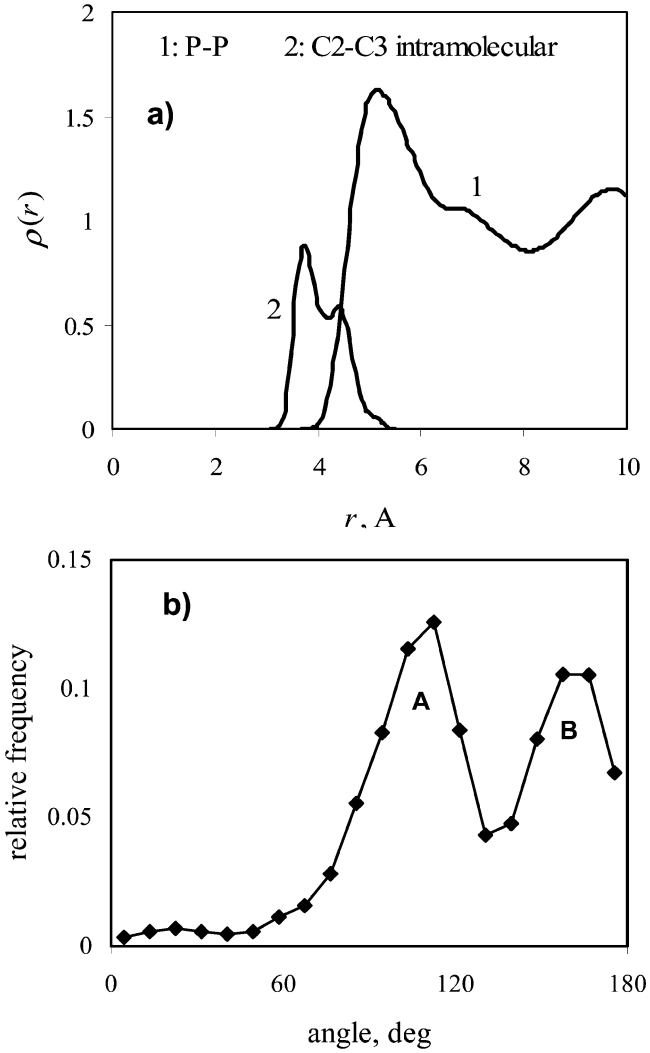

Figure 3. (a) Radial distribution functions in pure DMMP: (1) P−P RDF and (2) intramolecular contribution to C_2-C_3 RDF at 303 K. The first peak of the C_2-C_3 RDF corresponds to symmetric conformation A (Figure 2a), the second peak corresponds to asymmetric conformation B (Figure 2b). (b) The distribution of the $C_1-P_1-O_2-C_2$ torsion angle. The equilibrium angle is 109° for conformer A and 160° for conformer B.

Figure 4a shows the RDF in liquid DMMP. Naturally, the negatively charged oxygen atoms repel each other. On the other hand, the CH_3 groups are attracted to each other by strong van der Waals forces. Quite unexpected was a strong affinity of the CH_3 group attached to the central phosphorus atom to the oxygen that forms a double bond with the phosphorus. This correlation is strong enough to produce a secondary peak at 5.7 Å on the O_1-O_1 RDF.

4. DMMP−Water Solution

Simulation Details. Water was presented by a rigid three-center SPC/E model,[27] which reproduces quite accurately the

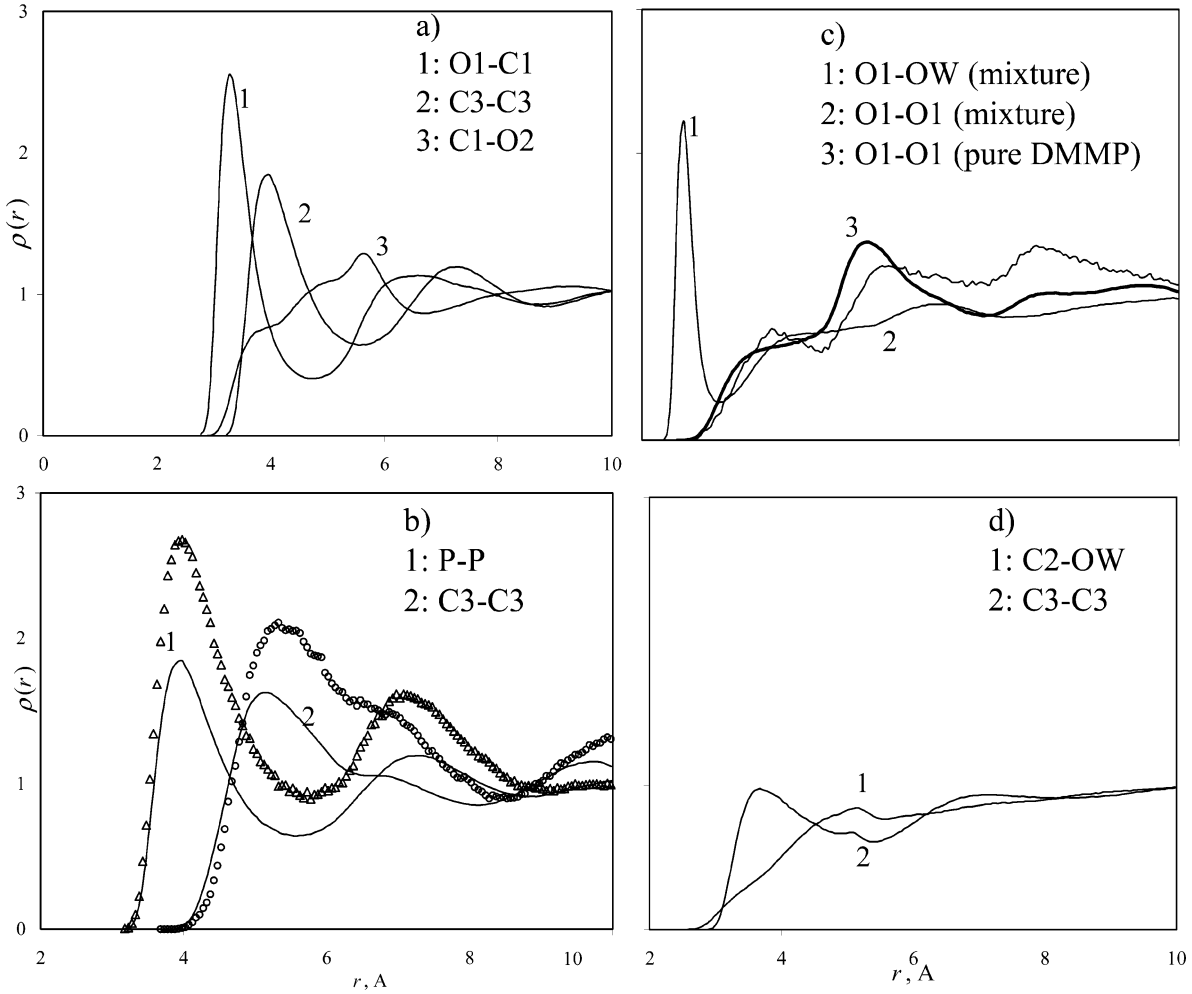

Figure 4. Radial distribution functions in pure liquid DMMP and mixture I (33 vol % DMMP solution in water) at 303 K: (a) pure DMMP; (b) comparison between P−P (1) and C3−C3 (2) RDFs for pure DMMP (symbols) and mixture (lines); (c) same for oxygen−oxygen RDFs (see legend); and (d) RDFs for the mixture.

density, the heat of evaporation, and the diffusion coefficient in pure water at ambient temperatures.[27] We explored three different compositions using model 1 (DMMP volume fraction of 25, 50, and 75%) and two compositions with model 2 (DMMP volume fraction of 33 and 50%). The simulation methods and details were the same as in simulations of pure DMMP (Section 3). The compositions and the resulting physical properties of the two mixtures are summarized in Table 4.

Phase Behavior and Thermodynamic Properties. Simulation with model 1 showed a phase segregation in the water−DMMP mixture. DMMP turned out to be immiscible with water, in apparent contradiction with the reality. The separation occurred at all three compositions (25, 50, and 75% vol). The wrong phase behavior is apparently caused by a low dipole moment of the DMMP molecule produced by the atomic charges of model 1.

On the contrary, model 2 predicted a hydrophilic solvation of DMMP in water with negative excess mixing volume and enthalpy, which is typical for two polar liquids that are able to form hydrogen bonds. For example, Figure 4b demonstrates that water prevails in the first solvation shell of DMP molecule, since RDFs for heavy DMMP atoms in solutions are lower than those in pure DMMP at short distances. From MD simulations of mixtures and pure components, we determined excess mixing volumes and enthalpies for the two compositions of 33 and 50% vol (Table 4). The excess thermodynamic functions are almost

TABLE 4: Simulated Systems and Physical Properties of Aqueous Solutions of DMMP with DMMP Volume Fraction of 33 and 50% Obtained from MD Simulations at 303 K

	mixture I	mixture II
N_{DMMP}	33	58
N_{H_2O}	396	342
volume fraction DMMP	0.332	0.503
mass fraction DMMP	0.365	0.539
mole fraction DMMP	0.077	0.145
ρ, g/cm^3	1.0674	1.0902
excess mixing volume $\Delta\tilde{V}_{mix}$, mL/mol	−0.36	−0.33
excess mixing volume, %	1.5%	1.1%
excess mixing enthalpy $\Delta\tilde{H}_{mix}$, kJ/mol	−0.19	−0.20
D_{DMMP}, cm^2/s (from MSD)	4.53 10^{-6}	
(from VACF)	4.57 10^{-6}	
D_{H2O}, cm^2/s (from MSD)	1.022 10^{-6}	
$\tau^{(rot)}_{DMMP}$, ps	9.8ps	
$\tau^{(rot)}_{H2O}$, ps	3.8ps	

equal at these two concentrations, that make us assume that their dependences on the composition have minima somewhere between 33 and 50% DMMP volume fraction. Many mixtures of hydrogen-bonding liquids exhibit minima in the intermediate concentration range, including some alchohols and dimethyl sulfoxide. As expected, the mobility of DMMP molecules in the mixture is higher than in the pure liquid, while the mobility of H_2O is substantially lower than that in the pure water. It

should be noted that the translation diffusion coefficients derived from MSD and VACF coincide nearly exactly (Table 4).

Hydrogen Bonding. In DMMP−water solution, water is able to donate and accept hydrogen bonds while DMMP only accepts hydrogen bonds with its three oxygen atoms. In this paper, hydrogen bonding was considered using geometric criteria that are applied commonly in molecular simulations; two oxygen atoms were considered to be connected by a hydrogen bond via a hydrogen atom if the distance between them did not exceed 3.4 Å and the (OHO) angle exceeded 120 degrees. As expected, the "ether" O_2 and O_3 atoms showed almost no ability to hydrogen bond (0.1 bond on average per atom), and the O_1 atom that forms a double bond with phosphorus and carries a larger negative charge of −0.69 showed significant ability to accept hydrogen bonds from water (1.5 bonds on average). On average, one DMMP molecule accepted 1.7 hydrogen bonds from water, that agrees well with the estimate of 2 bonds per DMMP molecule made in ref 28 from IR spectra. The ether-type oxygens, which do not show any considerable hydrogen bonding, do not even have a first peak on the RDFs with water oxygens. On the contrary, the O_1-O_W RDF exhibits a sharp peak due to hydrogen bonding (Figure 4c). Furthermore, the O_1-O_1 RDF is the solution differs qualitatively from that in pure DMMP (Figure 4c). The pronounced peak at 4 Å apparently corresponds to the other O_1 oxygen of DMMP, which forms a hydrogen bond with the same water molecule.

The lifetime of a hydrogen bond was estimated from the residence times of the water oxygen atom near the DMMP O_1 oxygen atom.[29] An average lifetime of 4.4 ps was obtained. This number is close to the water rotational correlation time τ_2 (Table 4), which means that complexes such as those typical for dimethyl sulfoxide−water mixtures[30] are not observed for DMMP.

Figure 4 shows the phosphorus−phosphorus and carbon−carbon radial distribution functions in 33% vol solution and pure DMMP at 303 K. The first peaks in the mixture are lower than in the pure liquid. This means that water prevails in the first solvation shell of the DMMP molecule.

5. Conclusion

In this paper, we have proposed a simple united-atom molecular model for DMMP. The model uses standard potential functions for both bonded and nonbonded interatomic interactions, which makes it easy to implement in standard software packages for molecular mechanics, molecular dynamics, and Monte Carlo simulations. The model is capable of reproducing accurately the ab initio and experimental data on the conformations of DMMP and physical properties of the pure liquid. By use of this model, we explored thermodynamic properties and molecular structure of aqueous solutions of DMMP by molecular dynamics simulations. It was shown that the accurate choice of partial charges is crucially important for correct description of thermodynamics of the mixture. On average, each DMMP molecule is found to form approximately two hydrogen bonds with water, but their lifetimes do not exceed the rotation correlation functions of individual water molecules, which indicates that no long-living DMMP·H_2O complexes are present in the aqueous solutions.

Acknowledgment. The authors thank D. Rivin for continuous interest and stimulating discussions. The work is supported by the US ARO, Grant DAAD190110545.

Supporting Information Available: C−P−O−C torsion potential function. This material is available free of charge via the Internet at http://pubs.acs.org.

References and Notes

(1) Frishman, G.; Amirav, A. *Field Anal. Chem. Technol.* **2000**, *4*, 170.
(2) Vo-Dinh, T.; Stokes, D. L. *Field Anal. Chem. Technol.* **1999**, *3*, 346.
(3) Suzin, Y.; Nir, I.; Kaplan, D. *Carbon* **2000**, *38*, 1129.
(4) Suenram, R. D.; Lovas, F. J.; Plusquellic, D. F.; Lesarri, A.; Kawashima, Y.; Jensen, J. O.; Samuels, A. C. *J. Mol. Spectrosc.* **2002**, *211*, 110.
(5) Arbuzov, B. A.; Vinogradova, V. S. *Izvestiya Akademii Nauk Sssr-Seriya Khimicheskaya* **1952**, 865.
(6) Arbuzov, B. A.; Shavsha, T. G. *Izv. Akad. Nauk Ser. Khim.* **1952**, 875.
(7) Kosolapoff, G. M. *J. Chem. Soc.* **1954**, 3222.
(8) Kosolapoff, G. M. *J. Am. Chem. Soc.* **1954**, *76*, 615.
(9) Barvik, I.; Stepanek, J.; Bok, J. *Czech. J. Phys.* **1998**, *48*, 409.
(10) Barvik, I.; Stepanek, J.; Bok, J. *J. Biomol. Struct. Dyn.* **2002**, *19*, 863.
(11) Bencsura, A.; Enyedy, I. Y.; Kovach, I. M. *J. Am. Chem. Soc.* **1996**, *118*, 8531.
(12) Soliva, R.; Monaco, V.; Gomez-Pinto, I.; Meeuwenoord, N. J.; Van der Marel, G. A.; Van Boom, J. H.; Gonzalez, C.; Orozco, M. *Nucleic Acids Res.* **2001**, *29*, 2973.
(13) Bencsura, A.; Enyedy, I.; Kovach, I. M. *Biochemistry* **1995**, *34*, 8989.
(14) Schlenkrich, M.; Brickmann, J.; MacKerell, A. D.; Karplus, M. An empirical potential energt function for phospholipids: criteria for parameter optimization and applications. In *Biological Membranes*; Merz, K., Roux, B., Eds.; Birkhauser: Boston, 1996; p 31.
(15) Weiner, S. J.; Kollman, P. A.; Case, D. A.; Singh, U. C.; Ghio, C.; Alagona, G.; Profeta, S.; Weiner, P. *J. Am. Chem. Soc.* **1984**, *106*, 765.
(16) Rappe, A. K.; Casewit, C. J.; Colwell, K. S.; Goddard, W. A.; Skiff, W. M. *J. Am. Chem. Soc.* **1992**, *114*, 10024.
(17) Gasteiger, J.; Marsili, M. *Tetrahedron* **1980**, *36*, 3219.
(18) Accelrys, I. Cerius2; 4.2 ed.; Accelrys Inc.: San Diego, CA, 2000.
(19) Buckingham, A. D.; Lefevre, R. J. W. *J. Chem. Soc.* **1952**, 1932.
(20) Arbuzov, B. A.; Vinogradova, V. S. *Izv. Akad. Nauk Ser. Khim.* **1952**, 505.
(21) Kaminski, G.; Duffy, E. M.; Matsui, T.; Jorgensen, W. L. *J. Phys. Chem.* **1994**, *98*, 13077.
(22) Lyubartsev, A. P.; Laaksonen, A. *Comput. Phys. Comm.* **2000**, *128*, 565.
(23) Verlet, L. *Phys. Rev.* **1967**, *159*, 98.
(24) vanGunsteren, W. F.; Berendsen, H. J. C. *Mol. Phys.* **1977**, *34*, 1311.
(25) Nose, S. *Mol. Phys.* **1984**, *52*, 255.
(26) Hoover, W. G. *Phys. Rev. A* **1985**, *31*, 1695.
(27) Berendsen, H. J. C.; Grigera, J. R.; Straatsma, T. P. *J. Phys. Chem.* **1987**, *91*, 6269.
(28) Eaton, G.; Harris, I.; Patel, K. *J. Chem. Soc., Faraday Trans.* **1992**, *88*, 3527.
(29) Vishnyakov, A.; Neimark, A. V. *J. Phys. Chem. B* **2000**, *104*, 4471.
(30) Luzar, A.; Chandler, D. *J. Chem. Phys.* **1993**, *98*, 8160.
(31) Laaksonen, L. gOpenMol; 2.0 ed.; CRC, Finnish IT centre for science: Espoo, Finland, 2001.
(32) Giotto, M. V.; Zhang, J.; Inglefield, P. T.; Wen, W. Y.; Jones, A. A. *Macromolecules* **2003**, *36*, 4397.